Promotion of Homologous Recombination and Genomic Stability by RAD51AP1 via RAD51 Recombinase Enhancement

***[1]Claudia Wiese, *[2]Eloïse Dray, [1]Torsten Groesser, [2]Joseph San Filippo, [2]Idina Shi, [1,4]David W. Collins, [1]Miaw-Sheue Tsai, [1]Gareth Williams, [1]Bjorn Rydberg, [2,3]Patrick Sung, and [1,3]David Schild**

[1]Life Sciences Division, Lawrence Berkeley National Laboratory, Berkeley, CA 94720, USA

[2]Department of Molecular Biophysics and Biochemistry, Yale University School of Medicine, New Haven, CT 06520, USA

[3]To whom correspondence should be addressed:

Patrick Sung: Department of Molecular Biophysics and Biochemistry, Yale University School of Medicine, C130 Sterling Hall of Medicine, 333 Cedar Street, New Haven, CT 06520.
Tel: 203-785 4569; Fax: 203-785 6037; E-mail: patrick.sung@yale.edu.

David Schild: Life Sciences Division, MS 74R0157, 1 Cyclotron Road, Lawrence Berkeley National Laboratory, Berkeley, CA 94720.
Tel: 510-486 6103; Fax: 510-486 6816; E-mail: dschild@lbl.gov

*These two authors have contributed equally to this study.

[4] Present address: Dept. of Ophthalmology, 10 Koret Way, UCSF, San Francisco, CA. 94143

Running title: RAD51AP1 Is Required for Homologous Recombination

SUMMARY

Homologous recombination (HR) repairs chromosome damage and is indispensable for tumor suppression in humans. RAD51 mediates the DNA strand pairing step in HR. RAD51AP1 (RAD51 Associated Protein 1) is a RAD51-interacting protein whose function has remained elusive. Knockdown of RAD51AP1 in human cells by RNA interference engenders sensitivity to different types of genotoxic stress. Moreover, RAD51AP1-depleted cells are impaired for the recombinational repair of a DNA double-strand break and exhibit chromatid breaks both spontaneously and upon DNA damaging treatment. Purified RAD51AP1 binds dsDNA and RAD51, and it greatly stimulates the RAD51-mediated D-loop reaction. Biochemical and cytological results show that RAD51AP1 functions at a step subsequent to the assembly of the RAD51-ssDNA nucleoprotein filament. Our findings provide the first evidence that RAD51AP1 helps maintain genomic integrity via RAD51 recombinase enhancement.

INTRODUCTION

In both prokaryotes and eukaryotes, homologous recombination (HR) represents a major DNA repair mechanism for the elimination of DNA double-strand breaks (DSB)s, inter-strand DNA crosslinks, and other types of deleterious chromosome lesions. HR that occurs early in meiosis is essential for tying homologous chromosomes together until time for their segregation in the first meiotic division (Symington, 2002; Sung and Klein, 2006). Interestingly, HR protein factors also play a role in telomere maintenance (McEachern and Haber, 2006). By virtue of its involvement in the repair of DNA damage and in other chromosome transactions, HR is indispensable for genomic integrity. Accordingly, deregulation or dysfunction in HR leads to chromosome fragility and, in humans, the cancer phenotype (Jasin, 2002; Surralles et al, 2004; Sung and Klein, 2006).

HR in mitotic cells is catalyzed by the RAD51 protein. Like its prokaryotic ortholog RecA, RAD51 polymerizes onto ssDNA to form a helical filament, called the presynaptic filament, and it catalyzes D-loop formation within the context of this filament. The recombinase activity of RAD51 is regulated by various protein-protein interactions (Symington, 2002; Sung and Klein, 2006).

Human RAD51AP1 (HUGO designation for PIR51) is a vertebrate-specific RAD51-interacting protein that was identified in a yeast two-hybrid library screen (Kovalenko et al., 1997). The mouse ortholog of RAD51AP1 (originally named RAB22) was identified in another yeast two-hybrid library screen (Mizuta et al., 1997). The RAD51-interaction domain resides within the C-terminus of RAD51AP1 (Kovalenko et al., 2006). Here, we show an involvement of RAD51AP1 in HR and the homology-directed repair of chromosome damage. Importantly, purified RAD51AP1 is found to interact specifically with and greatly enhance the recombinase activity of RAD51. Together, the genetic, cytological, and biochemical data presented herein establish RAD51AP1 as a novel HR factor that exerts its biological function through physical and functional interactions with RAD51.

RESULTS

RAD51AP1 Knockdown Causes DNA Damage Sensitivity and Chromatid Breaks

We used three different shRNAs to deplete the *RAD51AP1* transcript (see the Supplemental Results section and Fig. S1, A-C). Reproducibly, HeLa cells treated with all three *RAD51AP1* targeting shRNAs were significantly more sensitive (~2.3-fold based on D_{10} values) to mitomycin C (MMC) than cells not treated with any shRNA or with *GFP*-targeting shRNA or mutated shRNA #2 (Fig. 1A). The MMC-sensitivity of RAD51AP1-depleted HeLa cells was complemented by introducing the *EGFP RAD51AP1res* that is resistant to shRNA #2 (Fig. 1C). Because of the very transient expression/stability of the EGFP-RAD51 fusion protein, it was necessary to perform the complementation in a two-step process (see the Supplemental Material), and the apparent lack of complete complementation is most likely due to cells transfected with the shRNA #2 plasmid that were not transfected in the second round by EGFP-RAD51AP1res. RAD51AP1 knockdown also sensitized cells to the topoisomerase I poison camptothecin (CPT) (~1.6-fold; Fig. 1B) and cells in S-phase were mildly sensitized to X-rays (Fig. S2A).

RAD51AP1-depleted cells were tested for their level of chromatid breaks (ctbs), both spontaneously and after the induction of DNA damage. Following one acute 1 h exposure to 50 nM MMC, a 4- to 6-fold increase in ctbs was observed for RAD51AP1-depleted cells (Fig. 1D). In addition, significantly more spontaneous ctbs were present in the RAD51AP1-depleted cells (Fig. 1E). Following MMC treatment, we observed a ~4- to 5-fold increase in chromatid exchanges involving two or more chromosomes in cells upon RAD51AP1 knockdown (~0.5% in control cells, and ~2.5% and ~2.3% in cells depleted for RAD51AP1 by shRNA #2 and #3, respectively (Fig. 1F). Taken together, our results show that RAD51AP1 is necessary for the DNA damage repair and/or response in S-phase cells.

Involvement of RAD51AP1 in HR

We used our previously described TK6-neo-DRGFP cell line harboring the DR-GFP recombinational reporter (Wiese et al., 2002) to query whether RAD51AP1 has a role in HR. The reporter harbors a direct repeat of the mutant green fluorescent protein (GFP) gene. A site-specific DSB, generated in the upstream GFP copy by the I-*Sce*I endonuclease, triggers gene conversion with the downstream GFP copy to yield wild type GFP; flow cytometry was used to analyze the recombinant green fluorescent cells. TK6-neo-DRGFP cells were co-transfected with the I-*Sce*I expression plasmid and plasmids encoding shRNAs targeting either RAD51AP1 or XRCC3. As negative controls, we used a plasmid that codes for mutated shRNA #2 (which, as shown in Fig. S1D, is ineffective in extinguishing RAD51AP1 expression) and one that does not code for any shRNA. Reproducibly, knockdown of RAD51AP1 by either of two different shRNAs resulted in a ~2- to 2.5-fold decrease in HR (Fig. 2A and Fig. S3C), similar to what we observed for the knockdown of XRCC3 (Fig. 2A), which is known to be involved in HR (Pierce et al., 1999). As expected, neither of the two control plasmids had any effect. The 2- to 2.5-fold decrease in HR that we observe is comparable to that reported for siRNA-depletion of RAD51C (another RAD51 paralog) in HT1080 cells (Lio et al., 2004).

Deleted: do this

Deleted: expressing

Deleted: DNA damage

Deleted: treatmetn

Deleted:

Deleted: n

Deleted: 2.5-fold

Deleted: also

Deleted: and ??? S1F is a photo, but we may also show some data in a table in the supplement, or use 'data not shown')

Deleted: , and

Deleted: ?),

RAD51AP1 Interacts with RAD51 *In Vivo*

We found that upon X-ray treatment, ectopically expressed EGFP-RAD51AP1 co-localizes with RAD51 nuclear foci in U2OS cells, further supporting an involvement of RAD51AP1 in HR (Fig. S3A). Using EGFP-RAD51AP1 and HA-RAD51, and nuclear cell extracts from transfected HeLa cells, we found a co-immunoprecipitable complex of RAD51AP1 and RAD51 (Fig. S3B).

Deleted: S2

Deleted: ?).

RAD51AP1 Depletion Has No Effect on RAD51 Focus Formation

We asked whether X-ray-induced RAD51 focus formation is attenuated in cells with reduced levels of RAD51AP1, as some HR mutants show an impairment in this regard (Yuan et al., 1999; Bishop et al., 1998; van Veelen et al., 2005). However, whereas X-ray-induced RAD51 focus formation is reduced in HeLa cells depleted for either RAD51C or XRCC3, X-ray- and MMC-induced RAD51 foci assemble normally in HeLa cells depleted for RAD51AP1 (Fig. 2D and Fig. S3D).

Deleted: foci

Deleted: form

Deleted: ?).

Deleted: What if Reviewers ask to see X-ray sensitivity? Patrick, The X-ray data is now in Fig. S2A.

Purification of RAD51AP1

We added a cleavable GST-tag and a $(His)_6$-tag to the amino and carboxyl termini of RAD51AP1, respectively, and expressed the tagged protein in *E. coli*. The tagged RAD51AP1 is soluble, and a multi-step procedure was devised for its purification to near homogeneity (Fig. 3A). The GST portion of the purified protein can be removed using the PreScission protease. However, we used the uncleaved GST-tagged RAD51AP1 for biochemical analyses, as it shows no functional difference compared to RAD51AP1 without the GST tag (data not shown). Several independently purified RAD51AP1 preparations gave the same results in all the analyses.

Avid and Specific Interaction of RAD51AP1 with RAD51

An *in vitro* pulldown assay was employed to examine the ability of RAD51AP1 to interact with human RAD51. The *S. cerevisiae* Rad51 (yRad51) and *E. coli* RecA proteins were included as controls. Purified GST-tagged RAD51AP1 or GST was incubated with the recombinases, and glutathione Sepharose beads were used to capture any protein complex that had formed. The glutathione Sepharose beads were treated with SDS to elute the bound proteins, followed by SDS-PAGE analysis. All of the input RAD51 became associated with RAD51AP1 (Fig. 3B). The protein complex is highly specific, as little, if any, yRad51 or RecA was pulled down by RAD51AP1 (Fig. 3B and Fig. S4). As expected, none of the three recombinase proteins bound GST (Fig. 3B and Fig. S4). The above pulldown assay was done in the presence of a moderate level of salt (100 mM KCl), so we then asked whether the RAD51-RAD51AP1 complex can withstand higher salt levels. We saw little reduction in protein complex formation even at 500 mM KCl (Fig. S4). Taken together, the results from the pulldown assays revealed a highly specific and stable complex of RAD51AP1 and RAD51.

Deleted: ¶

DNA Binding by RAD51AP1

We used a DNA mobility shift assay with ^{32}P-labeled ssDNA and dsDNA as substrates to examine the DNA binding properties of RAD51AP1. RAD51AP1 appeared to have the same affinity for the two DNA species (Fig. 3C, panels I and II). However, when

RAD51AP1 was co-incubated with both DNA species, a distinct preference for dsDNA was revealed (Fig. 3C, panels III and IV). Half-maximal binding of dsDNA occurred at ~150 nM RAD51AP1, whereas ~400 nM of the protein was needed to attain half-maximal binding of the ssDNA species. Thus, we have been able to verify that RAD51AP1 binds both ssDNA and dsDNA (Kovalenko et al., 1997) and have provided evidence that it has a preference for dsDNA (Fig. 3C)

Enhancement of RAD51 Activity by RAD51AP1

During HR, a ssDNA substrate, derived from the processing of a DSB or another DNA lesion, is utilized by the recombination protein machinery to invade a homologous chromosome target to yield a DNA joint called the D-loop (Sung and Klein, 2006). We used an oligonucleotide based D-loop assay (Fig. 4A) to determine whether RAD51AP1 can enhance the RAD51-mediated DNA strand pairing reaction. Whereas only 2% of the input oligonucleotide was converted into D-loops by RAD51 (Fig. 4B, lane 3), the addition of RAD51AP1 enhanced the reaction by >10 fold. RAD51AP1 alone was incapable of D-loop formation, and, as expected (Sung and Klein, 2006), the reaction catalyzed by the combination of RAD51 and RAD51AP1 remains ATP-dependent (Fig. 4B, lane 6). The stimulatory effect of RAD51AP1 on RAD51 is highly specific, as no enhancement of the D-loop reaction catalyzed by either yRad51 (Fig. S5A) or RecA (data not shown) was seen.

Deleted: remained

ATP hydrolysis by RAD51 prompts the dissociation of the presynaptic filament (Bugreev and Mazin, 2004; Chi et al., 2006; Ristic et al., 2005). Because of this, the use of a non-hydrolyzable ATP analogue (e.g. AMP-PNP) or the RAD51 K133R protein (which binds but does not hydrolyze ATP) leads to the formation of a highly stable presynaptic filament (Bianco et al., 1998; Bugreev and Mazin, 2004; Chi et al., 2006; Cox, 2003; Ristic et al., 2005). Importantly, RAD51AP1 stimulated the D-loop forming ability of RAD51 K133R by a similar degree (Fig. 4C). When AMP-PNP was used as the nucleotide co-factor, the addition of RAD51AP1 again resulted in a marked enhancement of the D-loop reaction (Fig. S5B).

DISCUSSION

We have shown that cells depleted for RAD51AP1 are hypersensitive to a variety of chromosomal lesions, including DNA crosslinks, topoisomerase I-DNA adducts, and X-rays. Moreover, these cells exhibit an elevated level of spontaneous and DNA damage-induced chromatid breaks. We note that a recent study by a different group also documents that RAD51AP1-depleted cells are sensitized to MMC and have elevated MMC-induced chromatid breaks (Henson et al., 2006). The pattern of DNA damage sensitivity and chromosome fragility that accompany RAD51AP1 knockdown, and the association of RAD51AP1 with RAD51, suggest a role of this protein in chromosome damage repair via HR. Cytogenetic data and a direct test for HR efficiency using a recombination reporter have provided compelling evidence to support this premise.

For delineating the manner in which RAD51AP1 modulates the activity of RAD51, we have devised procedures for its expression and purification. We have verified that RAD51AP1 interacts with RAD51, but, interestingly, found that it does not associate with yRad51 or *E. coli* RecA. Our DNA binding studies have revealed a distinct

Deleted: ¶

preference of RAD51AP1 for dsDNA. Moreover, in an accompanying manuscript, Modesti et al (2007) present data to show that RAD51AP1 has an even higher affinity for branched DNA structures. Importantly, using the D-loop assay, we show a dramatic enhancement of the RAD51 DNA strand pairing activity by RAD51AP1. Since RAD51AP1 has no effect on the recombinase activity of yRad51 and RecA, it seems likely that its functional interaction with RAD51 is dependent on complex formation with the latter. This premise is supported by the use of a truncated RAD51AP1 variant that is incapable of RAD51 interaction in the D-loop assay (Modesti et al, 2007). The biochemical results that we have presented here, in conjunction with the available genetic and cell biological data, help establish a role of RAD51AP1 in HR and homology-directed DNA repair via enhancement of the RAD51 recombinase activity.

Assembly of the RAD51 presynaptic filament is a most critical step in HR, as all the biochemical steps that lead to D-loop formation occur within the confines of this filament (Bianco and Kowalczykowski, 1998; Symington, 2002; Sung et al., 2003; Sung and Klein, 2006). Cells deficient in the tumor suppressor BRCA2, any of the five RAD51 paralogs (RAD51B, RAD51C, RAD51D, XRCC2, and XRCC3), or SWS1 are impaired for the formation of RAD51 DNA repair foci, which likely correspond to presynaptic filaments of RAD51 (Symington, 2002; Martin et al., 2006). Studies involving the RAD51B-RAD51C complex, *Ustilago maydis* Brh2 (a BRCA2-like molecule), and a polypeptide derived from human BRCA2, have provided direct evidence that the RAD51 paralogs and BRCA2 function in the assembly of the RAD51 presynaptic filament, by aiding in the displacement of the single-strand DNA binding protein RPA from ssDNA (Sigurdsson et al., 2001a; Yang et al., 2005 ; San Filippo et al., 2006; Sung and Klein, 2006). Our results suggest that RAD51AP1 functions at a stage in the HR reaction subsequent to the assembly of the presynaptic filament, as (1) the frequency of RAD51 DNA repair foci is not affected by RAD51AP1 knockdown, and (2) under conditions wherein the RAD51 presynaptic filament is stable, RAD51AP1 still exerts a strong stimulatory effect on the D-loop reaction.

We note that *rad54* mutants are compromised for HR and, like RAD51AP1-deficient cells, show no defect in RAD51 focus formation (van Veelen et al., 2005). Rad54 protein possesses a robust DNA-dependent ATPase activity and it enhances the DNA strand pairing activity of RAD51 via ATP-hydrolysis driven alterations in the topology of duplex DNA (Van Komen et al., 2000; Ristic et al., 2001; Sung et al., 2003). Since RAD51AP1 does not possess any ATPase activity (data not shown), it must influence the RAD51-mediated homologous pairing reaction via a different mechanism.

Since only a partial depletion of RAD51AP1 can be accomplished by RNA interference, it seems very likely that HR and homology-directed DNA repair are much more dependent on RAD51AP1 than can be revealed in our cell-based experiments. The fact that the RAD51-mediated D-loop reaction shows a strong dependence on RAD51AP1 supports this premise. Interestingly, *RAD51AP1* expression levels seem to be altered in aggressive lymphoma and other cancers and, similar to *RAD51*, its expression level is cell cycle regulated (Song et al., 2004; Henson et al., 2006). It will be important to determine whether or not altered expression of RAD51AP1 contributes to the acquisition of the tumor phenotype.

Deleted: ¶

EXPERIMENTAL PROCEDURES

Deleted: E

Protein- and shRNA-encoding Plasmids, Transfection, Cell Culture MMC Treatment of Cells

The details are provided in the Supplemental Section.

Analyses of Chromosomal Aberrations

HeLa cells were treated with colcemid (100 ng/ml) for 4 h, detached from the culture vessel, washed in PBS and allowed to swell in 75 mM KCl at 37°C for 10 min. Cells were treated with methanol:acetic acid (3:1), dropped on wet slides, air dried, and stained in 3% Giemsa solution in Sørensen phosphate buffer for 10 min. Slides were covered with mounting media (Vectashield 60) and analyzed with a Zeiss Axioskop using a 100× lens with oil and 2000× magnification. We analyzed 50 to 100 metaphases in each case. Gaps were counted as a chromatid break (ctb) when the gap size was wider than the chromatid.

Indirect Immunofluorescence

Cells grown on four-well slides were treated with 8 Gy X-rays 3 days after transfection with the shRNA encoding plasmids and 1 day after transfection with the EGFP-RAD51AP1 encoding plasmid, and fixed with 4% paraformaldehyde at room temperature for 20 min. Cells were permeabilized with 0.5% Triton X-100 in PBS for 20 min, washed in PBS, blocked in 0.3% BSA in PBS overnight, and incubated with primary antibody to RAD51 (H-92; Santa Cruz; 1:1000; or ab213; Abcam; 1:1000) or primary antibody to GFP (ab290; Abcam; 1:1000) at 4°C overnight. After further washes with PBS, the cells were incubated for 1 h with Alexa Fluor 488 goat anti-rabbit IgG or Alexa Fluor 594 goat anti-mouse IgG (4 μg/ml). DNA was stained by DAPI (50 ng/ml). The slides were viewed at 2000× magnification in a Zeiss Axioskop microscope.

Recombination Assay and Flow Cytometry

The TK6-neo-DRGFP cell line (clone 1-7) has been described elsewhere (Wiese et al., 2002). I-SceI was expressed transiently from the pCβAsce expression vector (Richardson et al., 1998) and co-transfected with the plasmids encoding the shRNA, as indicated. Forty μg of each plasmid were used to transfect 4×10^6 cells suspended in 650 μl opti-MEM medium (Invitrogen) by electroporation (625 V/cm, 950 μF). Transfected cells were kept in regular growth medium for 24 h and then maintained in regular growth medium containing 100 μg/ml hygromycin B for 2 days. Transfected cells were analyzed by flow cytometry 3 days after electroporation to measure the percentage of cells expressing GFP (Wiese et al., 2002).

RAD51AP1 Expression and Purification

The details are provided in the Supplemental Section.

Other Recombination Proteins

RAD51 and yRad51 were purified as described previously (Sigurdsson et al., 2000b; Sung and Stratton, 1996). RecA protein was a kind gift from Michael Cox.

Pulldown Assay
RAD51 (4 µg), yRad51 (4 µg), or RecA (10 µg) was incubated with either GST (4 µg) or GST-RAD51AP1 (4 µg) in 30 µl of buffer B (20 mM KH_2PO_4, pH 7.4, 0.5 mM EDTA, 1 mM dithiothreitol, 0.01% Igepal CA-630, 100 mM KCl, and 10% glycerol) for 30 min at 4^oC. The reaction mixtures were mixed with 10 µl of glutathione-Sepharose beads (Amersham Biosciences) at 4°C for 30 min. After washing the beads twice with 30 µl of the same buffer, bound proteins were eluted with 30 µl of 2% SDS. The supernatant (S; after the beads have been collected by centrifugation), wash (W), and SDS eluate (E), 8 µl each, were analyzed by 10% SDS-PAGE and Coomassie Blue staining.

DNA Binding Assay
RAD51AP1 (50-1,600 nM) was incubated with 30 nM of ssDNA or dsDNA in 10 µl of reaction buffer (50 mM Tris, pH 7.5, 100 mM KCl, 1 mM $MgCl_2$, 1 mM dithiothreitol and 100 mg/ml BSA) at 37°C for 5 min. The reaction mixtures were resolved in 10% polyacrylamide gels in TAE buffer (40 mM Tris acetate, pH 7.4, 0.5 mM EDTA) at 4°C, followed by gel drying and quantification by phosphorimaging analysis. The DNA substrates were gel purified ^{32}P-labeled 80-mer species (San Filippo et al., 2006).

D-loop Assay
This was conducted essentially as described (Chi et al., 2006). Briefly, the ^{32}P-labeled 90-mer oligonucleotide substrate (2.4 µM nucleotides) was incubated for 5 min at 37°C with RAD51 (0.8 µM) in 10.5 µl reaction buffer (35 mM Tris, pH 7.5, 1 mM dithiothreitol, 5 mM $MgCl_2$, 50 mM KCl, containing either 2 mM ATP or AMP-PNP). The indicated amount of RAD51AP1 was then added in 1 µl, followed by a 5-min incubation at 37°C. Following the addition of pBluescript replicative form I DNA (35 µM base pairs) in 1 µl, the reaction mixtures were incubated for 6 min at 37°C and then subject to agarose gel electrophoresis. The radiolabeled DNA species were visualized and quantified by phosphorimaging analysis. The same procedure was used to analyze the effect of RAD51AP1 on yRad51 or RAD51 K133R.

REFERENCES

Bianco, P. R., Tracy, R. B., and Kowalczykowski, S. C. (1998). DNA strand exchange proteins: a biochemical and physical comparison. Front Biosci *3*, D570-603.
Bishop, A. J., and Schiestl, R. H. (2001). Homologous recombination as a mechanism of carcinogenesis. Biochim Biophys Acta *1471*, M109-121.
Bishop, D. K., Ear, U., Bhattacharyya, A., Calderone, C., Beckett, M., Weichselbaum, R. R., and Shinohara, A. (1998). Xrcc3 is required for assembly of Rad51 complexes in vivo. J Biol Chem *273*, 21482-21488.
Bugreev, D. V., and Mazin, A. V. (2004). Ca2+ activates human homologous recombination protein Rad51 by modulating its ATPase activity. Proc Natl Acad Sci U S A *101*, 9988-9993.
Chi, P., Van Komen, S., Sehorn, M. G., Sigurdsson, S., and Sung, P. (2006). Roles of ATP binding and ATP hydrolysis in human Rad51 recombinase function. DNA Repair (Amst) *5*, 381-391.

Cox, M. M. (2003). The bacterial RecA protein as a motor protein. Annu Rev Microbiol *57*, 551-577.
Henson, S. E., Tsai, S. C., Malone, C. S., Soghomonian, S. V., Ouyang, Y., Wall, R., Marahrens, Y., and Teitell, M. A. (2006). Pir51, a Rad51-interacting protein with high expression in aggressive lymphoma, controls mitomycin C sensitivity and prevents chromosomal breaks. Mutat Res *601*, 113-124.
Jasin, M. (2002). Homologous repair of DNA damage and tumorigenesis: the BRCA connection. Oncogene *21*, 8981-8993.
Kovalenko, O. V., Golub, E. I., Bray-Ward, P., Ward, D. C., and Radding, C. M. (1997). A novel nucleic acid-binding protein that interacts with human rad51 recombinase. Nucleic Acids Res *25*, 4946-4953.
Kovalenko, O. V., Wiese, C., and Schild, D. (2006). RAD51AP2, a novel vertebrate- and meiotic-specific protein, shares a conserved RAD51-interacting C-terminal domain with RAD51AP1/PIR51. Nucleic Acids Res *34*, 5081-5092.
Lio, Y. C., Schild, D., Brenneman, M. A., Redpath, J. L., and Chen, D. J. (2004). Human Rad51C deficiency destabilizes XRCC3, impairs recombination and radiosensitizes S/G2-phase cells. J Biol Chem 279: 42313-42320,.
Martin, V., Chahwan, C., Gao, H., Blais, V., Wohlschlegel, J., Yates, J. R., 3rd, McGowan, C. H., and Russell, P. (2006). Sws1 is a conserved regulator of homologous recombination in eukaryotic cells. Embo J *25*, 2564-2574.
McEachern, M. J., and Haber, J. E. (2006). Break-induced replication and recombinational telomere elongation in yeast. Annu Rev Biochem *75*, 111-135.
Mizuta, R., LaSalle, J. M., Cheng, H. L., Shinohara, A., Ogawa, H., Copeland, N., Jenkins, N. A., Lalande, M., and Alt, F. W. (1997). RAB22 and RAB163/mouse BRCA2: proteins that specifically interact with the RAD51 protein. Proc Natl Acad Sci U S A *94*, 6927-6932.
Modesti, M., Budzowska, M., Baldeyron, C., Demmers, J. A. A., Ghirlando, R., and Kanaar, R. (2007). RAD51AP1 is a structure-specific DNA binding protein that stimulates joint molecule formation during RAD51-mediated homologous recombination. Co-submitted to Mol. Cell.
Pierce, A. J., Johnson, R. D., Thompson, L. H., and Jasin, M. (1999). XRCC3 promotes homology-directed repair of DNA damage in mammalian cells. Genes Dev *13*, 2633-2638.
Pierce, A. J., Stark, J. M., Araujo, F. D., Moynahan, M. E., Berwick, M., and Jasin, M. (2001). Double-strand breaks and tumorigenesis. Trends Cell Biol *11*, S52-59.
Richardson, C., Moynahan, M. E., and Jasin, M. (1998). Double-strand break repair by interchromosomal recombination: suppression of chromosomal translocations. Genes Dev *12*, 3831-3842.
Ristic, D., Modesti, M., van der Heijden, T., van Noort, J., Dekker, C., Kanaar, R., and Wyman, C. (2005). Human Rad51 filaments on double- and single-stranded DNA: correlating regular and irregular forms with recombination function. Nucleic Acids Res *33*, 3292-3302.
Ristic, D., Wyman, C., Paulusma, C., and Kanaar, R. (2001). The architecture of the human Rad54-DNA complex provides evidence for protein translocation along DNA. Proc Natl Acad Sci U S A *98*, 8454-8460.

San Filippo, J., Chi, P., Sehorn, M. G., Etchin, J., Krejci, L., and Sung, P. (2006). Recombination mediator and Rad51 targeting activities of a human BRCA2 polypeptide. J Biol Chem *281*, 11649-11657.
Sigurdsson, S., Trujillo, K., Song, B., Stratton, S., and Sung, P. (2001a). Basis for avid homologous DNA strand exchange by human Rad51 and RPA. J Biol Chem *276*, 8798-8806.
Sigurdsson, S., Van Komen, S., Bussen, W., Schild, D., Albala, J. S., and Sung, P. (2001b). Mediator function of the human Rad51B-Rad51C complex in Rad51/RPA-catalyzed DNA strand exchange. Genes Dev *15*, 3308-3318.
Song, H., Xia, S. L., Liao, C., Li, Y. L., Wang, Y. F., Li, T. P., and Zhao, M. J. (2004). Genes encoding Pir51, Beclin 1, RbAp48 and aldolase b are up or down-regulated in human primary hepatocellular carcinoma. World J Gastroenterol *10*, 509-513.
Stark, J. M., Pierce, A. J., Oh, J., Pastink, A., and Jasin, M. (2004). Genetic steps of mammalian homologous repair with distinct mutagenic consequences. Mol Cell Biol *24*, 9305-9316.
Sung, P., and Klein, H. (2006). Mechanism of homologous recombination: mediators and helicases take on regulatory functions. Nat Rev Mol Cell Biol *7*, 739-750.
Sung, P., Krejci, L., Van Komen, S., and Sehorn, M. G. (2003). Rad51 recombinase and recombination mediators. J Biol Chem *278*, 42729-42732.
Sung, P., and Stratton, S. A. (1996). Yeast Rad51 recombinase mediates polar DNA strand exchange in the absence of ATP hydrolysis. J Biol Chem *271*, 27983-27986.
Symington, L. S. (2002). Role of RAD52 epistasis group genes in homologous recombination and double-strand break repair. Microbiol Mol Biol Rev *66*, 630-670, table of contents.
Van Komen, S., Petukhova, G., Sigurdsson, S., Stratton, S., and Sung, P. (2000). Superhelicity-driven homologous DNA pairing by yeast recombination factors Rad51 and Rad54. Mol Cell *6*, 563-572.
van Veelen, L. R., Essers, J., van de Rakt, M. W., Odijk, H., Pastink, A., Zdzienicka, M. Z., Paulusma, C. C., and Kanaar, R. (2005). Ionizing radiation-induced foci formation of mammalian Rad51 and Rad54 depends on the Rad51 paralogs, but not on Rad52. Mutat Res *574*, 34-49.
Wiese, C., Pierce, A. J., Gauny, S. S., Jasin, M., and Kronenberg, A. (2002). Gene conversion is strongly induced in human cells by double-strand breaks and is modulated by the expression of BCL-x(L). Cancer Res *62*, 1279-1283.
Yang, H., Li, Q., Fan, J., Holloman, W. K., and Pavletich, N. P. (2005). The BRCA2 homologue Brh2 nucleates RAD51 filament formation at a dsDNA-ssDNA junction. Nature *433*, 653-657.
Yuan, S. S., Lee, S. Y., Chen, G., Song, M., Tomlinson, G. E., and Lee, E. Y. (1999). BRCA2 is required for ionizing radiation-induced assembly of Rad51 complex in vivo. Cancer Res *59*, 3547-3551.

ACKNOWLEDGMENTS

We thank Dr. O. Kovalenko for RAD51AP1 material and Hector Nolla (Flow Cytometry Facility, UC Berkeley) for his help with flow cytometry. This work was supported by DOE Low Dose grant 441E, LBNL LDRD grant, NASA grant NNJ05HI36I, Public

Health Service grants RO1CA110415, RO1ES015252, and P01CA92584, and Susan G. Komen postdoctoral fellowship PDF0503471.

Deleted: 2

Deleted: 0 CHECK

FIGURE LEGENDS

Figure 1. Induction of MMC and CPT Sensitivity and Chromatid Breaks by RAD51AP1 Knockdown

(A and B) Survival curves of RAD51AP1-depleted cells to MMC and Camptothecin. Non-depleting negative controls: pRNAi, *GFP* shRNA and mutated shRNA #2. *shRNA #1 was tested in triplicate but with 2 μM MMC only, and resulted in the same sensitization as shRNA #2 and #3.

(C) Complementation of RAD51AP1-depletion in HeLa cells. Cells expressing both shRNA #2 and EGFP-RAD51AP1res. are more resistant to MMC than cells expressing mutated shRNA #2. All points with error bars represent the average of at least three different experiments ± 1 SD.

(D and E) MMC-induced and spontaneous chromatid breaks in RAD51AP1-depleted cells. Mutated shRNA #2 is a non-depleting negative control. Error bars: ± 1 SE for two (D) or three (E) independent experiments.

(F) Giemsa-stained metaphase spread of MMC-treated RAD51AP1-depleted HeLa cells. Black arrows: chromatid breaks; red arrow: chromatid exchange.

Figure 2. RAD51AP1-Depletion Impairs Homologous Recombination but not RAD51 DNA repair foci

(A) TK6-DRGFP cells depleted for RAD51AP1 (shRNA #2 or shRNA #3) or XRCC3 show ~2-to 2.5-fold lower levels of GFP+ cells (i.e. homologous recombinants) than control cells (transfected with either pRNAi or mutated shRNA #2). Data are the mean of the relative fraction of GFP+ cells from 5-7 independent experiments ± 1 SE (see also Fig. S3C).

Deleted: S2A

(B and C) Western blot analyses to show the extent of EGFP-RAD51AP1 (here:AP1)-depletion (B) or XRCC3 (here:X3)-depletion (C) in TK6-DRGFP cells. Two hairpins were tested for each gene (lanes 2 and 3 corresponding to shRNA #2 and shRNA #3, respectively) and compared to control cells (lanes 1: transfected with mutated shRNA #2). QM: loading control.

(D) RAD51 foci form normally in RAD51AP1-depleted HeLa cells after 8 Gy X-rays. Control transfected HeLa cells (mutated shRNA #2; panels A and B) and RAD51AP1-depleted cells (panels C-F) display bright RAD51 foci in ~ 80 % of the cells analyzed. In contrast, HeLa cells depleted for either RAD51C (panels G and H) or XRCC3 (panels I and J) show impaired RAD51 foci formation (i.e. only some cells form overall smaller and less intense RAD51 foci). Cells were fixed and stained at 8 h after 8 Gy X-rays. Two panels for each sample from different areas of the chamber slide are shown.

Figure 3. RAD51AP1 Purification and Characterization

(A) RAD51AP1 purification procedure (panel I). In panel II, extracts from cells before (lane 1) and after (lane 2) IPTG induction and purified RAD51AP1 (4 μg in lane 3) were analyzed by SDS-PAGE and Coomassie Blue staining.

(B) GST-tagged RAD51AP1 or GST was incubated with RAD51 or yRad51 and glutathione Sepharose beads were used to capture any protein complex that had formed. The beads were washed and treated with SDS to elute the bound proteins. The supernatant (S), wash (W) and SDS eluate (E) were analyzed by SDS-PAGE with Coomassie Blue staining.
(C) RAD51AP1 was incubated with either ssDNA (panel I), dsDNA (panel II), or both DNA species (panel III) and the mobility shift of the DNA substrates was analyzed in polyacrylamide gels. The results from panel III were plotted in panel IV.

Figure 4. Specific Enhancement of the RAD51-mediated D-loop Reaction by RAD51AP1
(A) Schematic of the D-loop assay.
(B) D-loop reactions mediated by RAD51 without or with RAD51AP1 (0.25 μM in lane 4 and 0.5 μM in lanes 5 and 6). ATP was omitted from the reaction in lane 6.
(C) D-loop reactions mediated by RAD51 K133R without or with RAD51AP1 (0.1, 0.25, 0.35, and 0.5 μM in lanes 4 to 7, respectively, and 0.6 μM in lanes 8 and 9). ATP was omitted from the reaction in lane 9. The results were plotted.

Figure 1

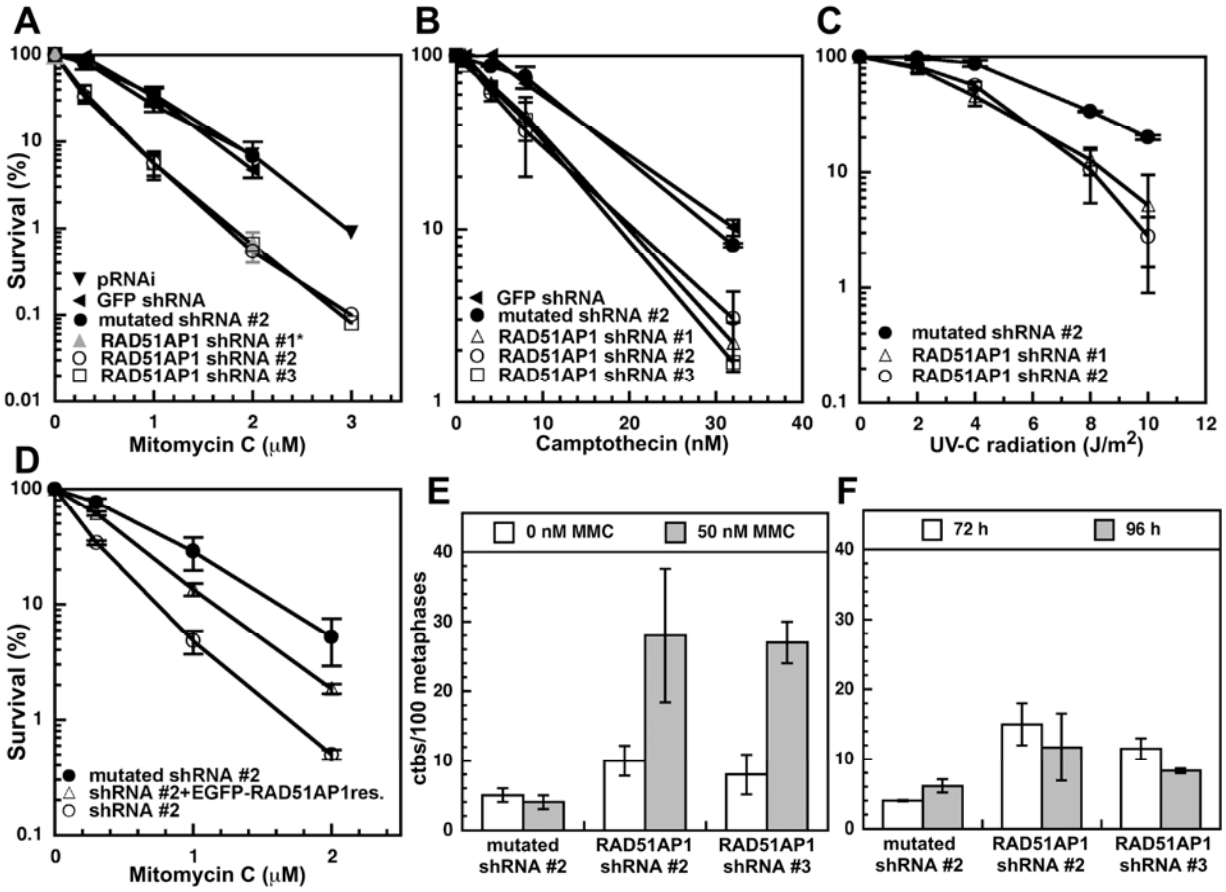
A
Survival (%)
Mitomycin C (μM)
pRNAi
GFP shRNA
mutated shRNA #2
RAD51AP1 shRNA #1*
RAD51AP1 shRNA #2
RAD51AP1 shRNA #3
B
Camptothecin (nM)
GFP shRNA
mutated shRNA #2
RAD51AP1 shRNA #1
RAD51AP1 shRNA #2
RAD51AP1 shRNA #3
C
UV-C radiation (J/m2)
mutated shRNA #2
RAD51AP1 shRNA #1
RAD51AP1 shRNA #2
D
Survival (%)
Mitomycin C (μM)
mutated shRNA #2
shRNA #2+EGFP-RAD51AP1res.
shRNA #2
E
ctbs/100 metaphases
0 nM MMC
50 nM MMC
mutated shRNA #2
RAD51AP1 shRNA #2
RAD51AP1 shRNA #3
F
72 h
96 h
mutated shRNA #2
RAD51AP1 shRNA #2
RAD51AP1 shRNA #3

Figure 2

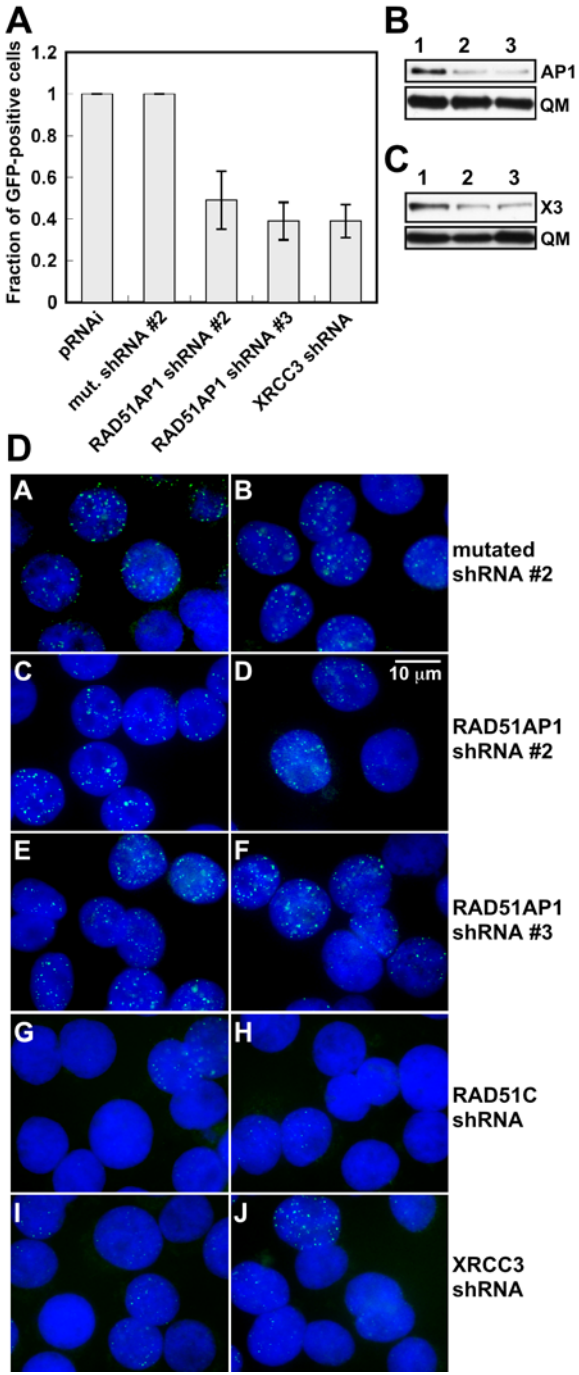
A
Fraction of GFP-positive cells
1.2
1
0.8
0.6
0.4
0.2
0
pRNAi
mut. shRNA #2
RAD51AP1 shRNA #2
RAD51AP1 shRNA #3
XRCC3 shRNA
B
1 2 3
AP1
QM
C
1 2 3
X3
QM
D
A
B
mutated shRNA #2
C
D
10 μm
RAD51AP1 shRNA #2
E
F
RAD51AP1 shRNA #3
G
H
RAD51C shRNA
I
J
XRCC3 shRNA

Figure 3

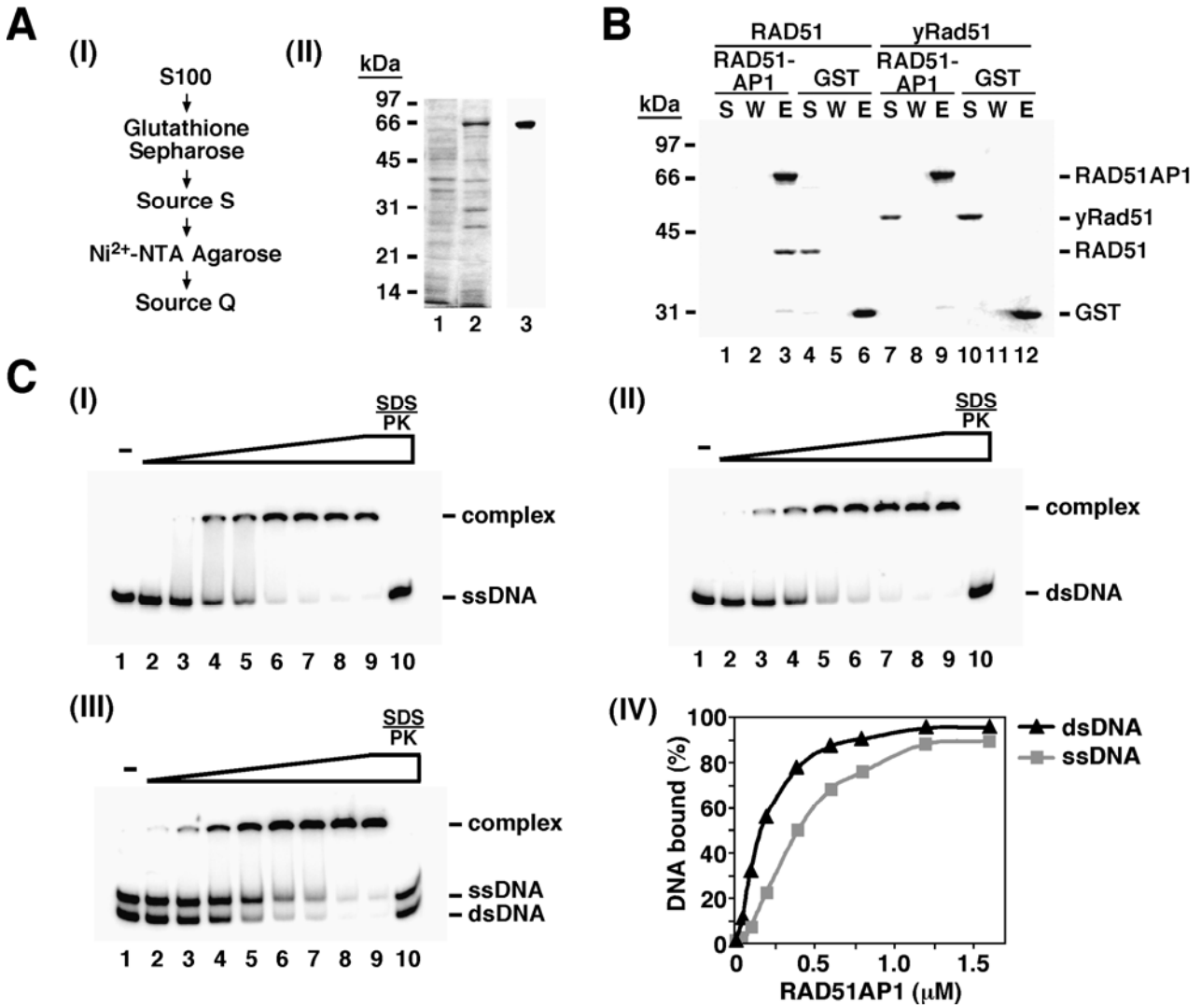
A
(I)
S100
Glutathione Sepharose
Source S
Ni2+-NTA Agarose
Source Q
(II)
kDa
97
66
45
31
21
14
1 2 3
B
RAD51
yRad51
RAD51-AP1
GST
RAD51-AP1
GST
kDa
S W E S W E S W E S W E
97
66
45
31
RAD51AP1
yRad51
RAD51
GST
1 2 3 4 5 6 7 8 9 10 11 12
C
(I)
SDS
PK
complex
ssDNA
1 2 3 4 5 6 7 8 9 10
(II)
SDS
PK
complex
dsDNA
1 2 3 4 5 6 7 8 9 10
(III)
SDS
PK
complex
ssDNA
dsDNA
1 2 3 4 5 6 7 8 9 10
(IV)
DNA bound (%)
100
80
60
40
20
0
0
0.5
1.0
1.5
RAD51AP1 (μM)
dsDNA
ssDNA

Figure 4

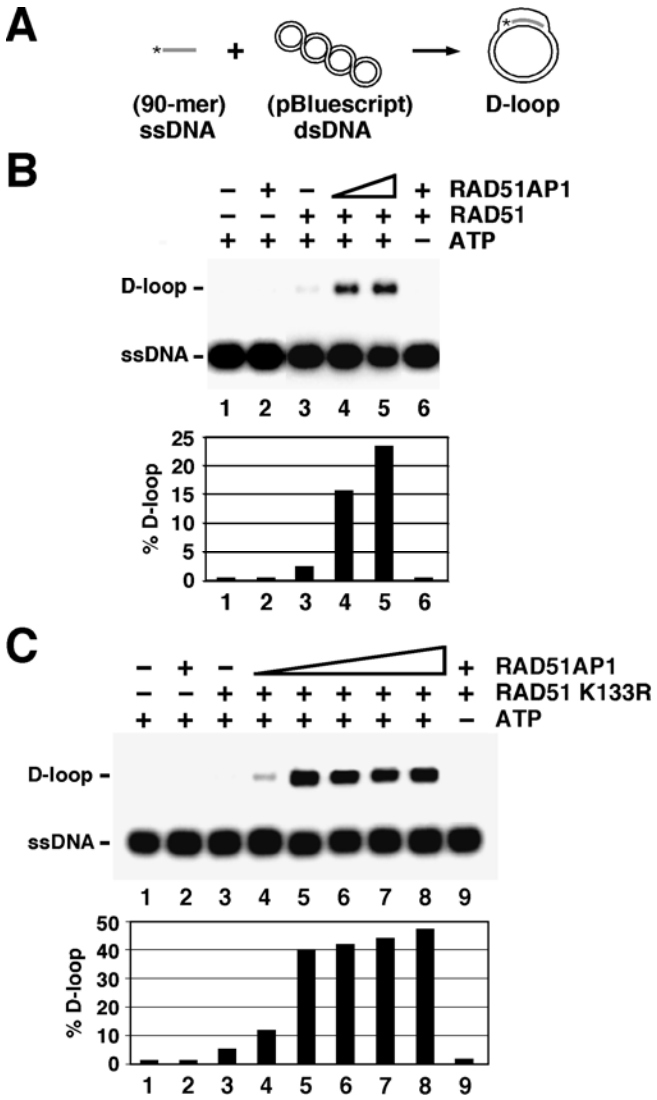
A
(90-mer) ssDNA
(pBluescript) dsDNA
D-loop
B
RAD51AP1
RAD51
ATP
D-loop
ssDNA
% D-loop
C
RAD51AP1
RAD51 K133R
ATP
D-loop
ssDNA
% D-loop

Figure S1

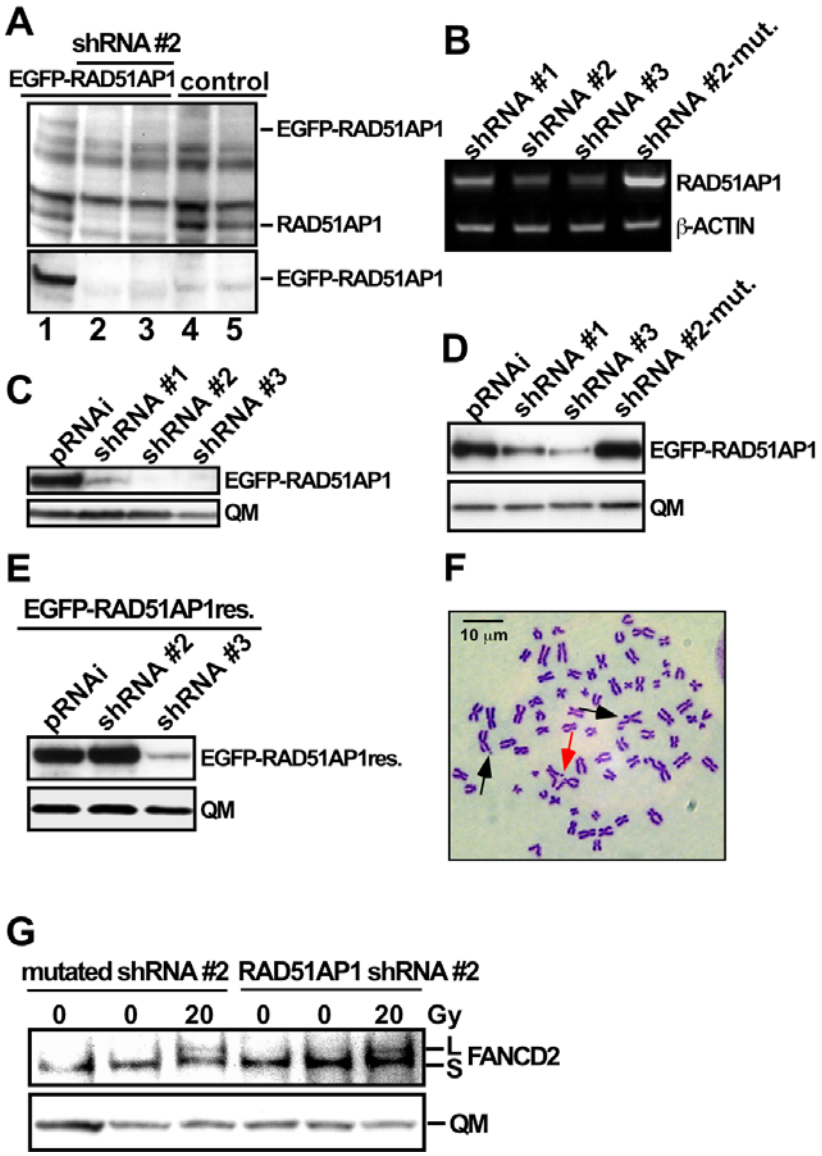
A
shRNA #2
EGFP-RAD51AP1
control
EGFP-RAD51AP1
RAD51AP1
EGFP-RAD51AP1
1 2 3 4 5
B
shRNA #1
shRNA #2
shRNA #3
shRNA #2-mut.
RAD51AP1
β-ACTIN
C
pRNAi
shRNA #1
shRNA #2
shRNA #3
EGFP-RAD51AP1
QM
D
pRNAi
shRNA #1
shRNA #3
shRNA #2-mut.
EGFP-RAD51AP1
QM
E
EGFP-RAD51AP1res.
pRNAi
shRNA #2
shRNA #3
EGFP-RAD51AP1res.
QM
F
10 μm
G
mutated shRNA #2
RAD51AP1 shRNA #2
0 0 20 0 0 20 Gy
L
S
FANCD2
QM

Figure S2

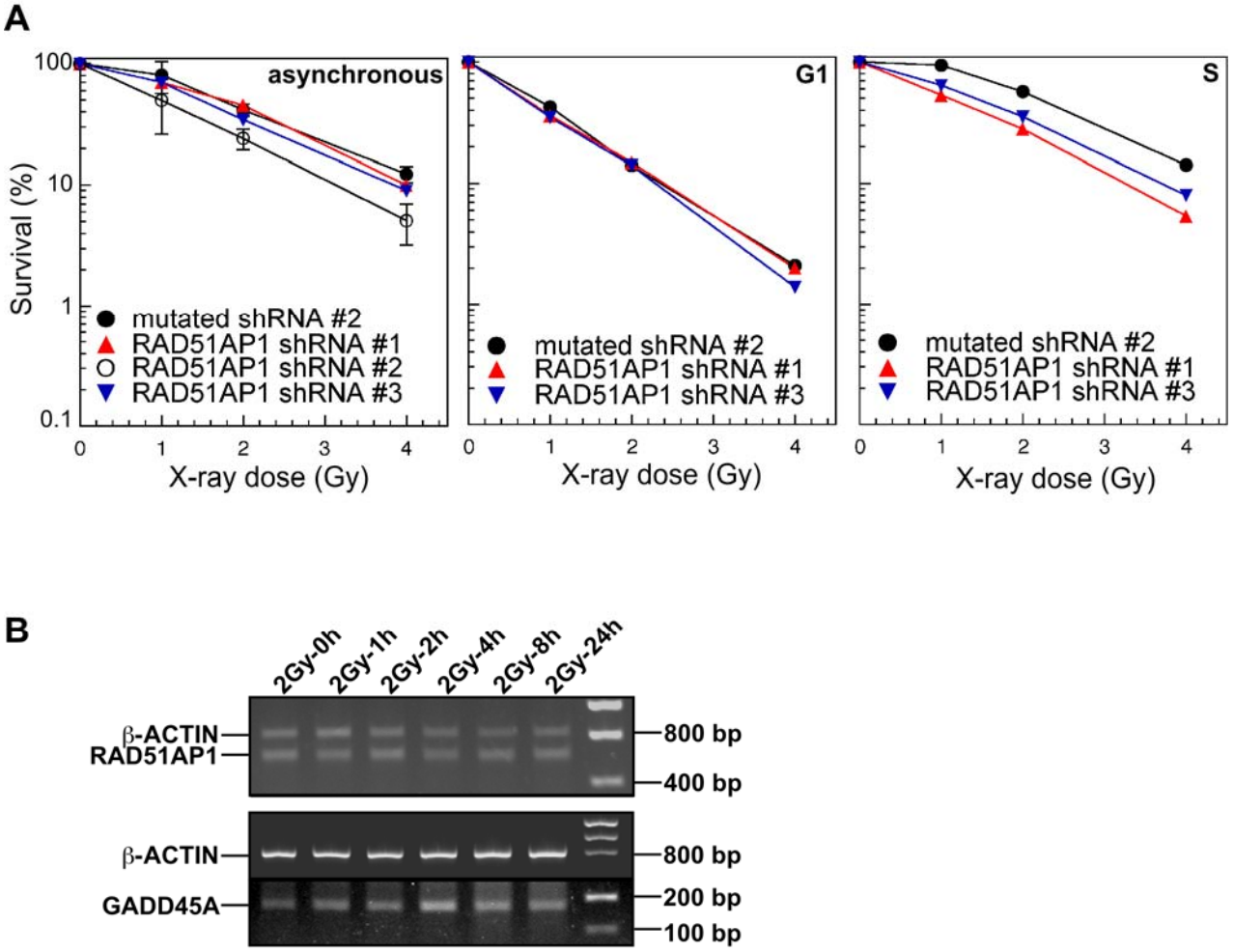
A
asynchronous
G1
S
Survival (%)
100
10
1
0.1
0
1
2
3
4
X-ray dose (Gy)
mutated shRNA #2
RAD51AP1 shRNA #1
RAD51AP1 shRNA #2
RAD51AP1 shRNA #3
B
2Gy-0h
2Gy-1h
2Gy-2h
2Gy-4h
2Gy-8h
2Gy-24h
β-ACTIN
RAD51AP1
800 bp
400 bp
β-ACTIN
GADD45A
800 bp
200 bp
100 bp

Figure S3

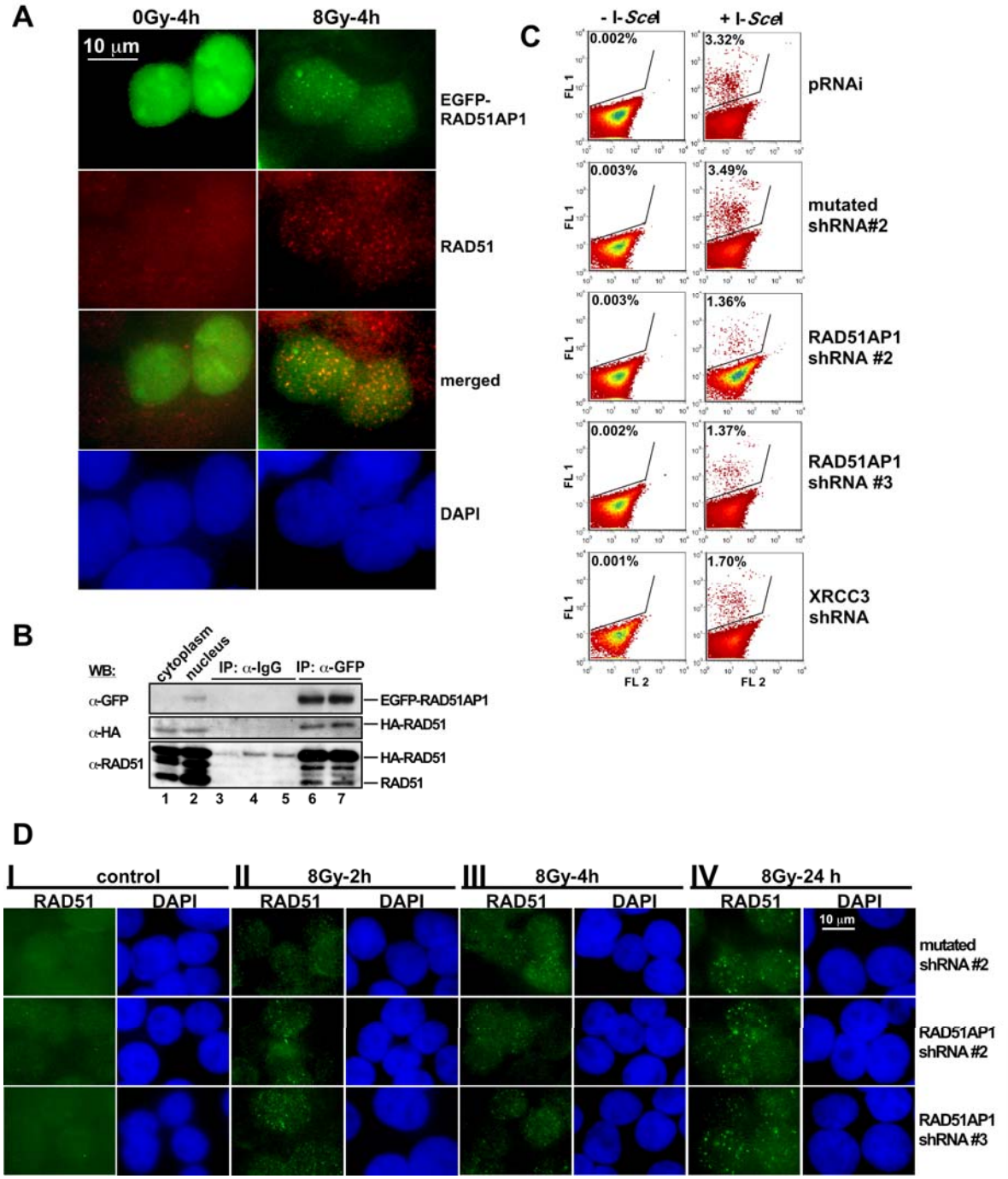
A
0Gy-4h
8Gy-4h
10 μm
EGFP-RAD51AP1
RAD51
merged
DAPI
B
WB:
cytoplasm
nucleus
IP: α-IgG
IP: α-GFP
α-GFP
α-HA
α-RAD51
EGFP-RAD51AP1
HA-RAD51
HA-RAD51
RAD51
1 2 3 4 5 6 7
C
- I-SceI
+ I-SceI
0.002%
3.32%
pRNAi
0.003%
3.49%
mutated shRNA#2
0.003%
1.36%
RAD51AP1 shRNA #2
0.002%
1.37%
RAD51AP1 shRNA #3
0.001%
1.70%
XRCC3 shRNA
FL 1
FL 2
D
I control
II 8Gy-2h
III 8Gy-4h
IV 8Gy-24 h
RAD51
DAPI
10 μm
mutated shRNA #2
RAD51AP1 shRNA #2
RAD51AP1 shRNA #3

Figure S4

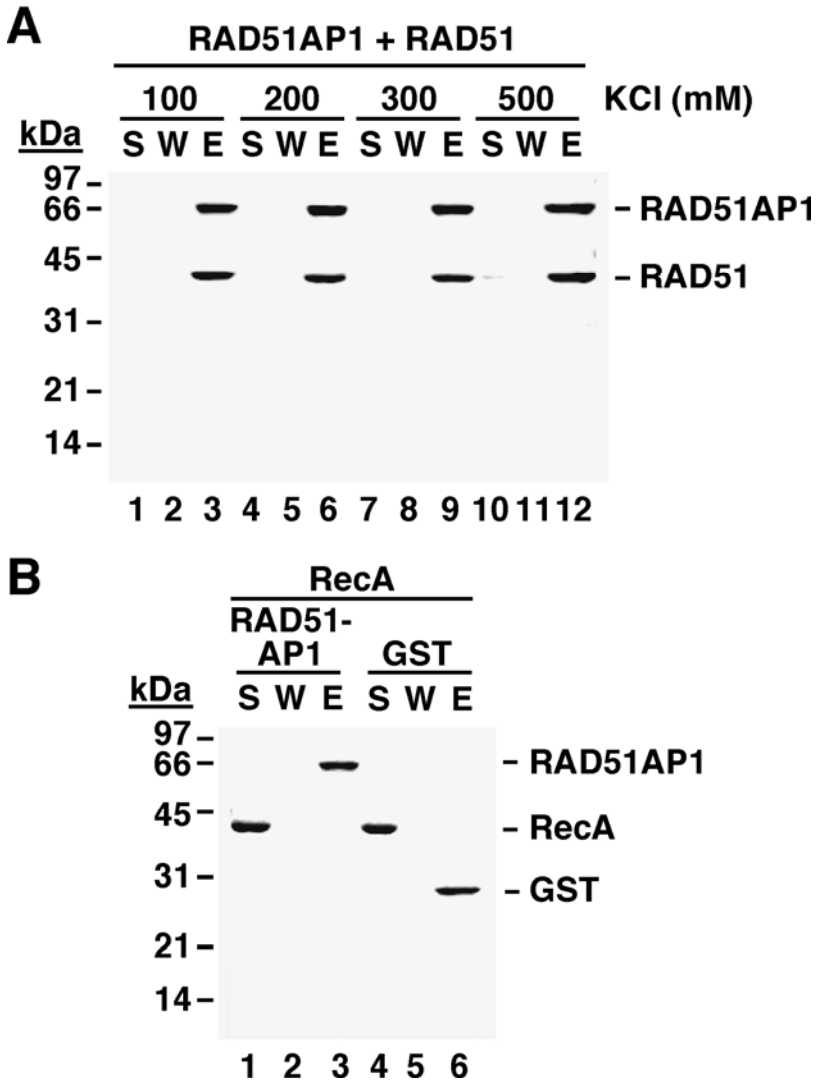
A
RAD51AP1 + RAD51
100
200
300
500
KCl (mM)
kDa
S W E S W E S W E S W E
97
66
45
31
21
14
RAD51AP1
RAD51
1 2 3 4 5 6 7 8 9 10 11 12
B
RecA
RAD51-AP1
GST
kDa
S W E S W E
97
66
45
31
21
14
RAD51AP1
RecA
GST
1 2 3 4 5 6

Figure S5

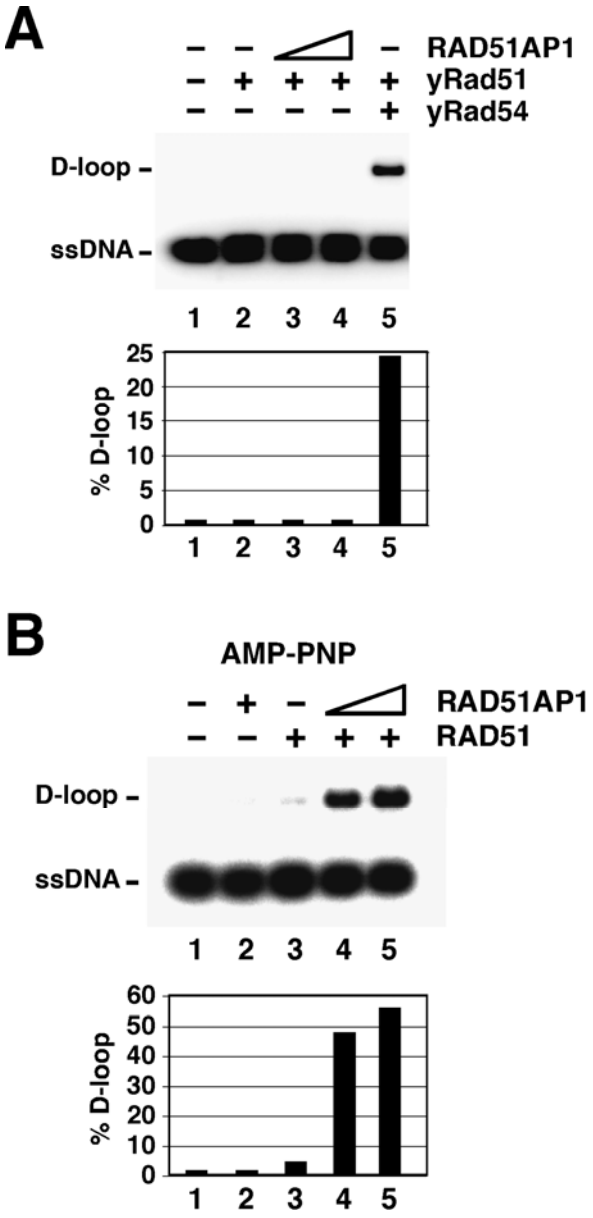
A
RAD51AP1
yRad51
yRad54
D-loop
ssDNA
1 2 3 4 5
% D-loop
25
20
15
10
5
0
1 2 3 4 5
B
AMP-PNP
RAD51AP1
RAD51
D-loop
ssDNA
1 2 3 4 5
% D-loop
60
50
40
30
20
10
0
1 2 3 4 5